# Architecture of the $Q_o$ Site of the Cytochrome $bc_1$ Complex Probed by Superoxide Production†

Florian L. Muller,‡,§ Arthur G. Roberts,‡,§ Michael K. Bowman,|| and David M. Kramer*,‡

*Institute of Biological Chemistry, Washington State University, 289 Clark Hall, Pullman, Washington 99164-6340, and WR Wiley Environmental Molecular Sciences Laboratory, Pacific Northwest National Laboratory, Richland, Washington 99352-0999*

*Received February 7, 2003; Revised Manuscript Received April 3, 2003*

ABSTRACT: Although several X-ray structures have been determined for the mitochondrial cytochrome (cyt) $bc_1$ complex, none yet shows the position of the substrate, ubiquinol, in the quinol oxidase ($Q_o$) site. In this study, the interaction of molecular oxygen with the reactive intermediate $Q_o$ semiquinone is used to probe the $Q_o$ site. It has been known for some time that partial turnover of the cyt $bc_1$ complex in the presence of antimycin A, a $Q_i$ site inhibitor, results in accumulation of a semiquinone at the $Q_o$ site, which can reduce $O_2$ to superoxide ($O_2^{\bullet-}$). It was more recently shown that myxothiazol, which binds close to the cyt $b_L$ heme in the proximal $Q_o$ niche, also induces $O_2^{\bullet-}$ production. In this work, it is shown that, in addition to myxothiazol, a number of other proximal $Q_o$ inhibitors [including (*E*)-*β*-methoxyacrylate-stilbene, mucidin, and famoxadone] also induce $O_2^{\bullet-}$ production in the isolated yeast cyt $bc_1$ complex, at ∼50% of the $V_{max}$ observed in the presence of antimycin A. It is proposed that proximal $Q_o$ site inhibitors induce $O_2^{\bullet-}$ production because they allow formation, but not oxidation, of the semiquinone at the distal niche of the $Q_o$ site pocket. The apparent $K_m$ for ubiquinol at the $Q_o$ site in the presence of proximal $Q_o$ site inhibitors suggests that the "distal niche" of the $Q_o$ pocket can act as a fully independent quinol binding and oxidation site. Together with the X-ray structures, these results suggest substrate ubiquinol binds in a fashion similar to that of stigmatellin with H-bonds between H161 of the Rieske iron−sulfur protein and E272 of the cyt *b* protein. When modeled in this way, mucidin and ubiquinol can bind simultaneously to the $Q_o$ site with virtually no steric hindrance, whereas progressively bulkier inhibitors exhibit increasing overlap. The fact that partial turnover of the $Q_o$ site is possible even with bound proximal $Q_o$ site inhibitors is consistent with the participation of two separate functional $Q_o$ binding niches, occupied simultaneously or sequentially.

The cytochrome (cyt)[1] $bc_1$ complex is a central enzyme in oxidative phosphorylation. It transfers electrons from ubiquinol ($UQH_2$) to cyt *c*, while shuttling protons into the mitochondrial intermembrane space (IMS). The proton motive force (*pmf*) generated by this process is then used to synthesize ATP (*1*, *2*). The mitochondrial complex is comprised of at least 11 subunits, but only three subunits appear to be catalytically important (*3*): the Rieske iron−sulfur protein (ISP), cyt $c_1$, and cyt *b* subunits. The ISP possesses a 2Fe−2S cluster, and cyt $c_1$ has a *c*-type heme. The cyt *b* protein possesses two cyt *b* hemes, cyt $b_H$ and cyt $b_L$, for their relatively high- and low-potential forms, respectively.

The cyt $bc_1$ complex has two distinct quinone/quinol binding sites. A binding site on the *n*-side (matrix) of the membrane reduces ubiquinone (UQ) during normal turnover and is known as the quinone reductase ($Q_i$) site. On the *p*-side or IMS side is a $UQH_2$ binding niche that oxidizes $UQH_2$ and is known as the quinol oxidase ($Q_o$) site.

Recently determined X-ray crystal structures of mitochondrial cyt $bc_1$ complexes demonstrated that the $Q_o$ site possesses proximal and distal $Q_o$ site niches (*4*, *5*). The proximal $Q_o$ niche is located close to the cyt $b_L$ heme, while the distal niche is located close to the ISP (*5*). The two niches bind different classes of inhibitors (*4*−*6*). Stigmatellin and 5-*n*-undecyl-6-hydroxy-4,7-dioxobenzothiazole (UHDBT) (*7*−*9*), which strongly interact with the Rieske ISP and bind at the distal niche (*5*), are termed distal $Q_o$ site inhibitors (*6*). MOA-stilbene (*10*), mucidin (strobilurin A) (*11*, *12*), famoxadone (*13*), and myxothiazol (*9*) bind closer to cyt $b_L$

† This work was supported by U.S. Department of Energy Grant DE-FG03-98ER20299 and a Frasch Foundation award (D.M.K.) and NIGMS Grant GM61904 (M.K.B.). The WR Wiley Environmental Molecular Sciences Laboratory is a national scientific user facility sponsored by the Department of Energy's Office of Biological and Environmental Research and located at Pacific Northwest National Laboratory.

* To whom correspondence should be addressed: Institute of Biological Chemistry, Washington State University, Pullman, WA 11964-6340. Telephone: (509) 335-4964. Fax: (509) 335-7643. E-mail: dkramer@wsu.edu.

‡ Washington State University.

§ These authors contributed equally to this work.

|| Pacific Northwest National Laboratory.

[1] Abbreviations: cyt, cytochrome; ISP, iron−sulfur protein; Mn-SOD, manganese-containing superoxide dismutase; MOA, (*E*)-*β*-methoxyacrylate; MOPS, 3-(*N*-morpholino)propanesulfonic acid; $Q_i$ site, ubiquinone reduction site; $Q_o$ site, ubiquinol oxidase site; $O_2^{\bullet-}$, superoxide; SOD, superoxide dismutase; SQ, (ubi)semiquinone; UHDBT, 5-*n*-undecyl-6-hydroxy-4,7-dioxobenzothiazole; UQ, ubiquinone; UQ-10, ubiquinone-10; UQ-20, ubiquinone-20; $UQH_2$, ubiquinol; $UQH_2$-1, ubiquinol-1; $UQH_2$-10, ubiquinol-10; $UQH_2$-20, ubiquinol-20.

10.1021/bi0342160 CCC: $25.00 
Published on Web 05/10/2003

(*4*, *6*) and are termed proximal $Q_o$ site inhibitors. Most models of quinol oxidation at the $Q_o$ site attribute functional significance to the two binding niches, either allowing for two quinoid species (i.e., UQ, ubisemiquinone, or $UQH_2$) to bind simultaneously (*14*, *15*) or allowing the semiquinone intermediate to pass from the distal to the proximal niche (*16*).

The Q-cycle, first formulated more than 20 years ago (*17*, *18*) and since modified by several groups (see, for example, refs *16*, *19*, and *20*), has gained widespread acceptance as the catalytic mechanism of the cyt $bc_1$ complex. Several independent X-ray structures of the cyt $bc_1$ complex strongly support this general model (*3*, *21*−*23*). In the Q-cycle, oxidation of $Q_o$ site-bound $UQH_2$ is a bifurcated process. The first $UQH_2$ electron is transferred through the high-potential chain, which includes the Rieske ISP and cyt $c_1$, leaving a reactive ubisemiquinone (SQ). The SQ then transfers an electron to the so-called low-potential chain, which includes two *b*-type hemes. Two protons from $UQH_2$ are released into the IMS (*p*-side of the membrane) upon quinol oxidation, possibly via H161 of the Rieske iron−sulfur protein (ISP) and E272 of the cyt *b* protein (*15*). The electron on cyt $b_L$ is then passed on to cyt $b_H$, and subsequently reduces UQ at the $Q_i$ site, forming a stabilized SQ. After a second turnover at the $Q_o$ site, the SQ at the $Q_i$ site is reduced to $UQH_2$, taking up two protons in the process. The net result of the Q-cycle is that four protons are transferred to the *p*-side of the membrane per two electron transfers from $UQH_2$ to cyt *c*.

There are at least four bypass reactions that must be controlled (*24*) to achieve the observed high yields of bifurcated electron transfer (*24*−*27*): (1) oxidation of $UQH_2$ by two sequential electron transfer reactions to the 2Fe2S cluster, resulting in a single proton released on the *p*-side per electron transferred; (2) oxidation of ferrocytochrome ($Fe^{2+}$) $b_L$ by the unstable $Q_o$ site SQ, re-forming $UQH_2$; (3) escape of the SQ from the $Q_o$ site and its disproportionation in the membrane; and (4) reduction of $O_2$ by an unstable SQ, forming superoxide ($O_2^{\bullet-}$) (reviewed in ref *24*).

In this study, we measure $O_2^{\bullet-}$ production as a probe of the $Q_o$ site SQ. Previously, we confirmed that $O_2^{\bullet-}$ production is, indeed, induced in the purified cyt $bc_1$ complex by myxothiazol, but the rates are one-half to one-third of that of the antimycin A-treated cyt $bc_1$ complex (*24*). In the work presented here, we show that induction of $O_2^{\bullet-}$ is a general feature of proximal $Q_o$ site inhibitors. We also present data which show that $O_2^{\bullet-}$ and other reactive $O_2$ species originate in the distal $Q_o$ site niche. Our kinetic measurements lead us to propose a model of the architecture of the $Q_o$ site $UQH_2$ binding domain, and offer strong experimental support for cyt $bc_1$ models involving functional compartmentalization of the $Q_o$ site and with the distal $Q_o$ site serving as an independent quinol oxidase site.

## MATERIALS AND METHODS

*Materials.* Stigmatellin, myxothiazol, antimycin A, ubiquinone-10 (UQ-10), ubiquinone-20 (UQ-20), decylubiquinone (decyl-UQ), and bovine cyt *c* were purchased from Sigma-Aldrich. Famoxadone, MOA-stilbene, and mucidin were kindly provided by A. Crofts (University of Illinois, Urbana, IL).

*Cytochrome $bc_1$ Complex and $O_2^{\bullet-}$ Assays.* The yeast cyt $bc_1$ complex was purified and assayed as described in ref *24*. The relative rate of $O_2^{\bullet-}$ production in the isolated cyt $bc_1$ complex was measured fluorometrically via $H_2O_2$ formation in the presence of saturating levels of superoxide dismutase (SOD) using the Amplex red−horseradish peroxidase method (Molecular Probes, Eugene, OR) and equilibrated in room air (*24*). The assay was calibrated using $H_2O_2$ standards provided in the kit, under identical experimental conditions to account for any interference. In all cases, the background rates in the absence of the complex were subtracted from the enzymatic rates of $H_2O_2$ production. Consistent with the expected stoichiometry, the rate of $H_2O_2$ production was half that of $O_2^{\bullet-}$ (see below).

We also measured $O_2^{\bullet-}$ production by the SOD-sensitive reduction of cyt *c* (*28*, *29*), as described previously (*24*). The buffer and substrates [50 $\mu$M bovine cyt *c*, 50 $\mu$M decyl-ubiquinol (decyl-$UQH_2$), 1 mM KCN, 50 mM MOPS, and 100 mM KCl (pH 6.90)] were the same as those used for measuring cyt $bc_1$ activity. Decyl-$UQH_2$ was used for most experiments since it yielded the lowest background rates. However, key experiments were repeated using $UQH_2$-10 and $UQH_2$-20, as indicated.

*Molecular Modeling of Proximal $Q_o$ Inhibitors Bound with Ubiquinone at the $Q_o$ Site.* Using the alignment feature of DS Viewer Pro, version 5.0 (Accelrys, Inc., San Diego, CA), the stigmatellin-, myxothiazol-, famoxadone-, and MOA-stilbene-containing structures of the cyt $bc_1$ complex (*3*, *23*) were aligned with the cyt *b* hemes and the highly conserved PEWY sequence (reviewed in ref *30*) from each of the structures. In crystal structures, the position of the hydrophilic headgroup of the Rieske ISP is highly variable (*3*). For simplicity, we assume that distal $Q_o$ site occupants, such as $UQH_2$-1 and stigmatellin, orient the soluble head domain of the Rieske ISP into the same position. For the alignments, particular stringency was placed on the cyt *b* heme iron atoms because they scatter X-rays relatively well, giving more accurate positions. Also, the relative positions of these irons change little between cyt $bc_1$ complexes from different species, in different crystal forms, and with bound inhibitors (*2*, *23*, *31*). Ultimately, good structural overlaps were obtained in this way. The alignment was refined further using the backbone of E272 and the aromatic plane of W273 of the conserved PEWY sequence [bovine cyt $bc_1$ numbering (*3*)]. The resulting alignment allowed us to compare the $Q_o$ sites from the various structures and inhibitors.

The structure of a quinol substrate, ubiquinol-1 ($UQH_2$-1), was initially superimposed on the stigmatellin 6-methoxy-4-*o*-methylquinol group in the stigmatellin-bound cyt $bc_1$ X-ray structure (*3*). The $UQH_2$-1 headgroup was placed to minimize the distances between the OH groups of the hydroquinone and its two assumed (see below) H-bond acceptors: $\epsilon$-N of H161 of the ISP and E272 of cyt *b*.

No X-ray structure of the cyt $bc_1$ complex with mucidin bound has yet been published, but the structure of this inhibitor is very similar to that of MOA-stilbene; we thus used the MOA-stilbene structure as a template to predict its bound position.

The overlap between $Q_o$ site inhibitors and the hypothetical position of the $UQH_2$-1 was calculated using the molecular modeling package Vega (*32*). The overlapped volume was calculated by taking the sum of the individual volumes of

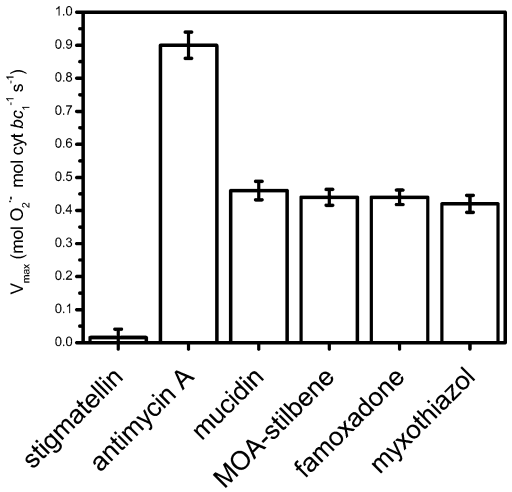


FIGURE 1: Dependence of $V_{max}$ for $O_2^{\bullet-}$ production on the nature of the inhibitor. The experimental conditions are described in Materials and Methods. The concentration of the inhibitors was 10 $\mu$M. In this figure, each bar represents the average of at least three experiments.

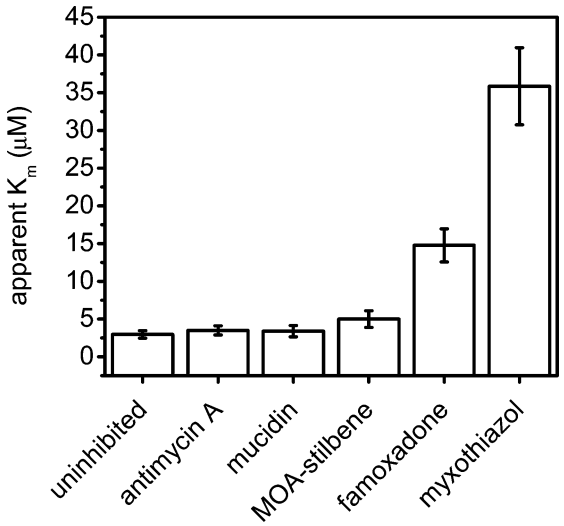


FIGURE 2: $K_m$ of decyl-$UQH_2$ as a function of inhibitor. The experimental conditions were as described for the $H_2O_2$ assay, with the exception of KCN being omitted, and the concentration of decyl-$UQH_2$ was varied from 8 to 100 $\mu$M, with five measurements per $K_m$ determination. The experiment was repeated at least twice for each inhibitor, and the data were analyzed via Eadie−Hofstead plots.

the respective $Q_o$ site inhibitor and $UQH_2$-1 and subtracting the total volume occupied by these structures in our model.

## RESULTS AND DISCUSSION

*$O_2^{\bullet-}$ Production by Proximal $Q_o$ Site Inhibitors.* Figure 1 shows the Amplex red fluorescent-detected $V_{max}$ of $O_2^{\bullet-}$ production in the isolated yeast cyt $bc_1$ complex with various inhibitor/substrate treatments. The highest rates of superoxide production were observed in the presence of antimycin A, where the $V_{max}$ (saturating decyl-$UQH_2$) was estimated to be 0.88 mol of $O_2^{\bullet-}$ (mol of cyt $bc_1$)$^{-1}$ $s^{-1}$. This reaction was essentially completely inhibited by addition of stigmatellin. In the presence of saturating concentrations of myxothiazol, mucidin, famoxadone, and MOA-stilbene induced superoxide production at ~50% of the rate induced by antimycin A, with an absolute rate of ~0.42 mol of $O_2^{\bullet-}$ (mol of cyt $bc_1$)$^{-1}$ $s^{-1}$ at saturating concentrations of decyl-$UQH_2$. Similar rates of $O_2^{\bullet-}$ production were observed with saturating concentrations of $UQH_2$-10 or $UQH_2$-20 instead of decyl-$UQH_2$ as a substrate (data not shown). Because the proximal niche inhibitors are predominantly noncompetitive with $UQH_2$ (*33*), we do not expect these levels of substrate to have displaced the inhibitors. Furthermore, addition of 4-fold higher concentrations of the $Q_o$ site inhibitors or co-addition of saturating levels of antimycin A had no effect on rates (data not shown), indicating that displacement of $Q_o$ site inhibitors followed by the normal Q-cycle did not occur.

Essentially no $O_2^{\bullet-}$ was detected with the uninhibited cyt $bc_1$ complex or in the absence of cyt *c* (data not shown).

We repeated these experiments using the SOD sensitive cyt *c* reduction by superoxide detection method (see Materials and Methods). We found that, just as reported earlier with myxothiazol (*24*), the cyt $bc_1$ complex treated with mucidin, famoxadone, and MOA-stilbene exhibited a residual rate of cyt *c* reduction, which could be inhibited by ~50% upon the addition of Mn-SOD. The $V_{max}$ values (data not shown) for superoxide production for the antimycin A-treated [~0.8 mol of $O_2^{\bullet-}$ (mol of cyt $bc_1^{-1}$) $s^{-1}$ at pH 6.90] or proximal $Q_o$ site inhibitor-treated [0.48 ± 0.05 mol of $O_2^{\bullet-}$ (mol of cyt $bc_1^{-1}$) $s^{-1}$ at pH 6.90] complex were almost identical to those measured by the Amplex red assay. As we reported for myxothiazol (*24*), addition of stigmatellin to the proximal $Q_o$ site inhibitor-treated cyt $bc_1$ complex completely eliminated $O_2^{\bullet-}$ production (data not shown).

Superoxide production in the presence of proximal $Q_o$ site inhibitors was unaffected by the addition of 10 $\mu$M antimycin A, indicating that the reductant of $O_2$ was not at the $Q_i$ site. Because proximal $Q_o$ site inhibitors prevent the reduction of cyt $b_L$, we can also exclude cyt $b_L$ as a site for superoxide production. We can also rule out the semiquinone formed by the equilibration of unbound quinone and quinol as a major source of superoxide, since $O_2^{\bullet-}$ production was undetected in the absence of the cyt $bc_1$ complex or cyt *c*. This leads us to suggest that the distal niche of the $Q_o$ site pocket is the site of $O_2^{\bullet-}$ production under the conditions described above. This is confirmed by the action of stigmatellin, a known distal niche $Q_o$ site inhibitor. Since the SQ is likely the only species that is sufficiently reducing to produce superoxide (reviewed in ref *34*), we hypothesize that proximal $Q_o$ site inhibitors allow the partial oxidation of substrate quinol to a semiquinone, but preventing its further oxidation, thus increasing the steady-state semiquinone concentration. Essentially the same explanation has been given for $O_2^{\bullet-}$ production induced by antimycin A (*35*), but with a few notable differences (see below).

The bulkiness of the $Q_o$ site proximal niche inhibitor affects the apparent $K_m$ for ubiquinol. We previously suggested that the proximal $Q_o$ site inhibitor, myxothiazol, may alter the properties of substrate binding to the $Q_o$ site (*24*). Indeed, the apparent $K_m$ for exogenously added decyl-$UQH_2$ assayed by $O_2^{\bullet-}$ production in the presence of myxothiazol was ~7-fold higher than that determined by either normal turnover or $O_2^{\bullet-}$ production in the presence of antimycin A (Figure 2). However, the overall bulkiness of the $Q_o$ site inhibitors appears to be quite important. Myxothiazol is the largest inhibitor that was studied, and produced the highest $K_m$ value ($K_m$ ~ 36 $\mu$M). Consistent

with the relative sizes of the proximal $Q_o$ site inhibitors, this is followed by famoxadone ($K_m$ = 15 $\mu$M), MOA-stilbene ($K_m$ = 5 $\mu$M), and mucidin ($K_m$ = 3 $\mu$M). Surprisingly, the decyl-$UQH_2$ $K_m$ value for $O_2^{\bullet-}$ production in the presence of mucidin was virtually indistinguishable from that in the presence of antimycin A or that for normal Q-cycle turnover. It appears that, in the presence of mucidin, the smallest proximal $Q_o$ site inhibitor, the distal $Q_o$ site niche retains the full affinity of a completely unoccupied $Q_o$ site, suggesting that mucidin and ubiquinol can bind simultaneously and independently. The experiments were repeated with $UQH_2$-10, instead of decyl-$UQH_2$, as the substrate and with mitochondrial membranes instead of the isolated cyt $bc_1$ complex. While the absolute $K_m$ values varied slightly under these conditions, the relative order of $K_m$ values (i.e., myxothiazol > famoxadone > MOA-stilbene > mucidin ~ antimycin A ~ normal turnover) remained the same (data not shown).

We expect that there are considerable species differences in how proximal $Q_o$ site inhibitors affect $O_2^{\bullet-}$ production by the cyt $bc_1$ complex on the basis of well-known differences in sensitivity to these inhibitors. We found that, in the isolated *Rhodobacter sphaeroides* cyt $bc_1$ complex, while both antimycin A and mucidin induced $O_2^{\bullet-}$ production, the larger $Q_o$ site inhibitors (myxothiazol, famoxadone, and MOA-stilbene) did not (F. L. Muller, A. R. Crofts, and D. M. Kramer, unpublished observations). This suggests that, in this species, the inhibitors bind somewhat differently, or the proximal and distal $Q_o$ niches overlap significantly.

*Defining the Bounds of the $Q_o$ Site Distal Niche*. As we noted previously (*24*), the maximal rate of $O_2^{\bullet-}$ production, with saturating decyl-$UQH_2$, was lower (~2-fold) in the presence of myxothiazol than in the presence of antimycin A (see Figure 1 and above). In this work, we show that the $V_{max}$ was nearly identical among the different proximal $Q_o$ site inhibitors. Because the $V_{max}$ (at saturating $UQH_2$) likely represents the rate of oxidation of bound $UQH_2$, this result suggests that the $UQH_2$ headgroup is bound at the $Q_o$ site in essentially the same position, regardless of the presence of the various proximal $Q_o$ site inhibitors. The simplest explanation for a constant $V_{max}$ but a varying $K_m$ is that quinol binding displaces the larger inhibitors or that conformational changes within the $Q_o$ pocket allow a very similar binding of the substrate.

We used computer-simulated "docking" to explore the location for binding of the substrate, $UQH_2$-1, at the $Q_o$ site (see Materials and Methods). Initially, the various inhibitors were left in the positions predicted or inferred from X-ray structures (see above), while the $UQH_2$-1 headgroup (shown in blue) was placed (see Materials and Methods) into the "stigmatellin position", with essentially the same position and orientation as the 6-methoxy-4-*o*-methylquinol group of stigmatellin, i.e., with ~3.0 Å H-bonds between H161 of the ISP and E272 of cyt *b* (data not shown). Extensive overlap was observed between $UQH_2$-1 and stigmatellin, as expected. It was qualitatively observed that increasing substrate−inhibitor overlap was seen when $UQH_2$-1 was docked into the stigmatellin position in structures with progressively bulkier proximal $Q_o$ site inhibitors. However, in this position, $UQH_2$-1 overlapped (overlap = 66 Å$^3$) significantly with mucidin, which would be inconsistent with the $K_m$ observed for mucidin (Figure 2 and data not shown).

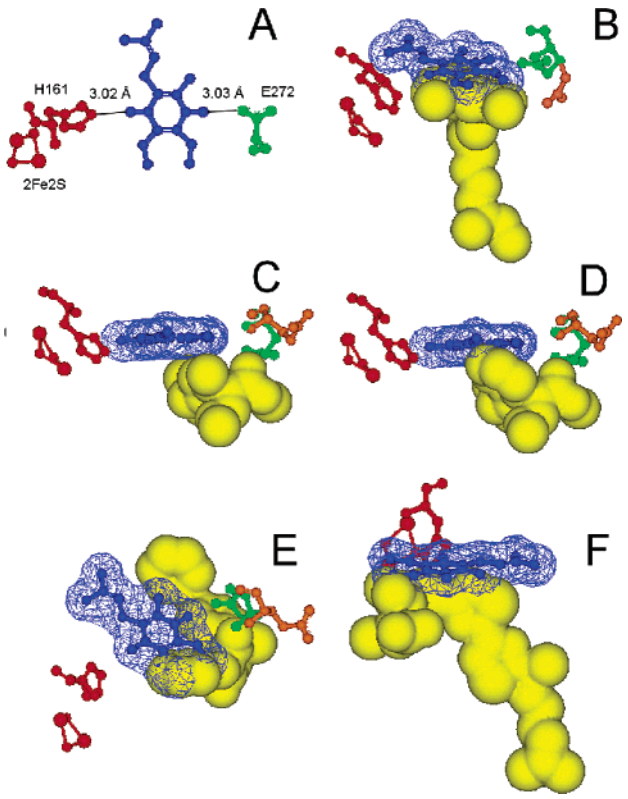


FIGURE 3: Modeling of proximal $Q_o$ site inhibitors with ubiquinone at the $Q_o$ site. Alignment of the cyt $bc_1$ X-ray crystal structures showing occupancy at the $Q_o$ site by the substrate, $UQH_2$-1 (blue), and $Q_o$ site inhibitors (yellow). E272 of cyt *b* is shown in its hypothetical position with $UQH_2$-1 (green) and $Q_o$ site inhibitor-shifted position (orange). Also shown are the 2Fe−2S cluster and H161 of the stigmatellin-inhibited cyt $bc_1$ X-ray crystal structure (red). (A) Bird's eye view of the $Q_o$ site, showing a ball-and-stick model of $UQH_2$-1 (blue), hydrogen bonds between H161 from the stigmatellin-inhibited cyt $bc_1$ X-ray crystal structure, and the hypothetical position of the E272 side chain. The $Q_o$ site shows a wire mesh van der Waals surface of $UQH_2$-1 (blue) and a solid van der Waals surface of (B) stigmatellin, (C) mucidin, (D) MOA-stilbene, (E) famoxadone, and (F) myxothiazol, showing their overlap. The $Q_o$ sites were oriented in different orientations to exemplify the overlap between $UQH_2$-1 and the $Q_o$ site inhibitors.

To resolve this contradiction, the $UQH_2$-1 was repositioned so that the overlap would be minimized between $UQH_2$-1 and mucidin. Figure 3 shows that the most straightforward solution was to pivot the carboxylate side group of E272 from stigmatellin-inhibited cyt $bc_1$ by 51° along the axis formed by the $C_\alpha-C_\beta$ bond, allowing $UQH_2$-1 to bind less than 3.0 Å from the original position inferred from the stigmatellin, while retaining H-bond lengths of ~3.0 Å between H161 and E272. It is notable that E272 (and the PEWY loop in general) is highly flexible and found in a number of positions in the different X-ray structures (*3*), and we feel that allowing this residue to move is reasonable. In this position, mucidin only exhibited a small overlap with $UQH_2$-1 of 5.2 Å$^3$ (Figure 3C). In this new position, $UQH_2$-1 has an overlap with stigmatellin and myxothiazol of 60.7 (Figure 3B) and 60.3 Å$^3$ (Figure 3F), respectively. The intermediate-sized inhibitors, famoxadone and MOA-stilbene, showed overlap of 51.1 (Figure 4E) and 23.3 Å$^3$ (Figure 3D). Consistent with the $K_m$ values that were observed, increasing substrate−inhibitor overlap was again seen when $UQH_2$-1 was docked into this position in structures with progressively bulkier proximal $Q_o$ site inhibitors (cf. Figures 2 and 3).

The fact that $V_{max}$ for $O_2^{\bullet-}$ production was similar in the presence of each of the inhibitors can be explained if both the proximal $Q_o$ site inhibitors and $UQH_2$-1 can bind simultaneously. We used the simulations to determine what it would take for the proximal $Q_o$ site inhibitors to bind simultaneously in the presence of the hypothetical $UQH_2$-1. In two cases, moving E272 involved breaking an H-bond. In the case of MOA-stilbene, a weak predicted H-bond from the inhibitor carbonyl and the amide proton of E272 was broken. In the case of famoxadone, the hydrogen bond between the oxygen of the oxazolidinedione group of famoxadone and the amide backbone proton of E272 was broken. Qualitatively, the breaking of H-bonds and the extents of PEWY loop rearrangements required to achieve good H-bonding with the substrate could also explain the observed differences in the $K_m$ values for $O_2^{\bullet-}$ production. We found other reasonable structural rearrangements, which could allow simultaneous binding of inhibitor and substrate. For example, the hydrophobic interaction of the phenylamino group of famoxadone could be disrupted, as suggested by its observed flexibility (*23*), rotating the group away from the distal $Q_o$ site niche to allow substrate binding. Alternatively, the substrate could rotate along the H161−E272 hydrogen bond axis, avoiding the phenylamino group of the inhibitor. Moreover, the soluble head domain of the Rieske ISP is known to be in a variety of conformations in different crystal structures (*2*, *36*). When this was taken into consideration, less manipulation of the inhibitors is required to achieve simultaneous binding of the inhibitor and $UQH_2$-1. At present, we do not have any data to distinguish these possibilities, but these simulations demonstrate the possibility of complete, and partially functional, double occupancy of the $Q_o$ pocket, as suggested by the kinetic data.

*Differences between Proximal and Distal $Q_o$ Site Inhibitors.* Proximal and distal inhibitors have been differentiated by the specific niches that they occupy in the $Q_o$ site niche (*2*). From the aligned X-ray crystal structures (see Materials and Methods), ~50% of the volume between the distal $Q_o$ site inhibitor stigmatellin (volume = 521.4 Å$^3$) and the proximal $Q_o$ site inhibitor myxothiazol (volume = 488.8 Å$^3$) overlaps (overlap volume = 200.7 Å$^3$), implying that the volumes occupied by proximal and distal niche $Q_o$ site inhibitors are not mutually exclusive. Stigmatellin forms relatively strong H-bonds with both H161 and E272, preventing interactions with substrate. This obviously explains the complete inhibition of $UQH_2$ oxidation by stigmatellin. On the other hand, myxothiazol has no H-bonds to the side groups of H161 and E272, but shifts the E272 side group away from the $Q_o$ site, a general feature of proximal $Q_o$ site inhibitors. Therefore, we suggest that these inhibitors are best differentiated by their binding mechanism, rather than by a more-or-less specific binding niche.

The above structural analysis offers a straightforward explanation for the observed noncompetitive behavior of $Q_o$ site inhibitors, as well as their ability to bind in the presence of substrate (*14*, *33*). Consistent with our results, Brandt and co-workers (*33*) noted that binding of substrate quinol changed the $K_D$ for certain proximal niche inhibitors by a small amount, a factor of ~2. This indicates that $Q_o$ site proximal niche inhibitors can bind simultaneously, at the same overall site, but their mutual interactions are rather small.

The results presented here may also have important implications for the energetics of the ISP head domain movements. The ISP head domain is found in different positions in crystal structures, depending upon a number factors, including the presence of different $Q_o$ site inhibitors (*23*, *37*, *38*). Binding of $Q_o$ distal niche inhibitors such as stigmatellin or 5-undecyl-6-hydroxyl-4,7-dioxobenzothiazole (UHDBT), which form hydrogen bonds to the His ligand of the 2Fe−2S cluster, tends to fix the ISP in the $ISP_B$ position (in the $Q_o$ pocket). On the other hand, certain $Q_o$ proximal niche inhibitors (MOA-stilbene and famoxadone) favor the "released" positions (i.e., those not at the $Q_o$ site) (*23*, *37*, *38*). Our results, and those of Brandt and co-workers (*33*), show that the $Q_o$ site proximal inhibitors and substrate can bind simultaneously. If $UQH_2$ indeed forms hydrogen bonds between E272 of cyt *b* and H161 of the ISP, then this mutual binding would require movement of the ISP head domain to the $ISP_B$ position. The relatively small effects of inhibitor binding on $K_M$ for $UQH_2$ (Figure 2) and of substrate binding on inhibitor $K_D$ (*33*) would imply a relatively small difference in free energy among the different $ISP_B$ positions in the native (not crystallized) complex, at least when induced by proximal niche inhibitors.

*Implications for Inhibitor-Induced $O_2^{\bullet-}$ Production in Mitochondria.* Several studies in intact mitochondria reported that myxothiazol inhibits $O_2^{\bullet-}$ production (*35*, *39*, *40*), in apparent contradiction with our results and those reported in refs *41* and *42*. Our data suggest an explanation for these results. Starkov et al. (*41*) noted that a high succinate-to-fumarate ratio was required for efficient myxothiazol $O_2^{\bullet-}$ production in mitochondria. The ratio of succinate to fumarate determines the redox state of the quinone pool via complex II. At a ratio of 1:20, the level of myxothiazol-induced $O_2^{\bullet-}$ production was low, whereas the level of antimycin A-induced $O_2^{\bullet-}$ production was high (*41*). This could be explained by the relatively high $K_m$ for quinol in the presence of myxothiazol since a higher concentration of ubiquinol would be required to saturate the site. Our measurements of the $K_m$ of ubiquinol for $O_2^{\bullet-}$ production support this explanation (Figure 2). Large proximal $Q_o$ site inhibitors (famoxadone and myxothiazol) have relatively large $K_m$ values for ubiquinol, indicating weak binding at the distal $Q_o$ site. On the other hand, the $K_m$ for $UQH_2$ was not really changed by smaller proximal $Q_o$ inhibitors (MOA-stilbene and mucidin), which molecular modeling indicates can bind almost unobstructed concomitantly with ubiquinol (Figure 3). Thus, when the amount of reduced substrate is small, myxothiazol and the large inhibitors could decrease the level of $O_2^{\bullet-}$ production by increasing the substrate $K_m$ above the concentration of the reduced substrate.

An obvious question about this work is whether our results are somehow an isolation artifact or are perhaps a consequence of the use of the artificial substrate, decyl-$UQH_2$. We note that proximal $Q_o$ site-induced $O_2^{\bullet-}$ production was also observed when $UQH_2$-10 or $UQH_2$-20 was used as the substrate (data not shown). In addition, myxothiazol, mucidin, MOA-stillbene, and famoxadone (as well as antimycin A) were also found to induce $O_2^{\bullet-}$ production in mitochondrial membranes supplemented with the more natural substrates succinate, $UQH_2$-10, and $UQH_2$-20 (data not shown). Furthermore, we were able to confirm that proximal $Q_o$ site inhibitors and antimycin A also induced $O_2^{\bullet-}$ production *in*

*vivo* in *S. cerevisiae*; these data will be published in a complementary paper (F. L. Muller and D. M. Kramer, manuscript in preparation).

*Implications for the Mechanism of Ubiquinol Oxidation and for Mutations of the $Q_o$ Site*. The fact that myxothiazol, mucidin, MOA-stilbene, and famoxadone can induce $O_2^{\bullet-}$ production in the isolated cyt $bc_1$ complex and *in vivo* indicates that quinol oxidation at the $Q_o$ site can proceed even if the proximal niche is blocked.

There are several important implications for $Q_o$ site catalysis arising from this basic conclusion. First, it appears that $UQH_2$ and proximal $Q_o$ site inhibitors can bind simultaneously to the $Q_o$ site. Two types of kinetic models can account for this behavior well. The model proposed by Crofts and co-workers (*15*) incorporates a single $Q_o$ site quinoid species that moves during catalysis. That quinol is first bound essentially in the distal niche of the $Q_o$ pocket. Only after partial oxidation and deprotonation does it move to the proximal niche. Within this model, our data suggest that the distal niche can operate independently of the proximal niche, but that its product is unable to transfer its electron to the cyt *b* heme, possibly because the semiquinone is unable to migrate to within range for rapid electron transfer.

In the mobile semiquinone models in the presence of antimycin A, both the distal and proximal binding niches are potentially open to the semiquinone intermediate. Addition of a proximal $Q_o$ site inhibitor would eliminate one of these niches. Given that the overall equilibrium constant for the formation of the semiquinone from-bound quinol is small, elimination of one of the two niches should lower the steady-state concentration of the semiquinone. If the reactivity of the semiquinones in the two niches were on the same order of magnitude, this could also account for the approximately 2-fold lower maximal rates of $O_2^{\bullet-}$ production with the proximal niche $Q_o$ site inhibitors with respect to that with antimycin A.

Models in which two quinoid species are simultaneously bound at the $Q_o$ site pocket have also been proposed (*20*, *43*, *44*). Our data could be accommodated in this type of model, provided that only one of the quinone species is specifically displaced by mucidin (the smallest of the proximal $Q_o$ site inhibitors). The fact that the $K_m$ for $UQH_2$ is unaffected by mucidin suggests that the remaining quinone species binds normally. This would preclude strong interaction between the two proposed quinone species. In this case, proximal $Q_o$ site inhibitors could induce $O_2^{\bullet-}$ production by blocking the normal oxidation of the reactive semiquinone. Alternatively, if the semiquinone electron is normally delocalized over two quinoid species, eliminating one should significantly lower the stability of the radical species.

Finally, with the finding that blocking the proximal $Q_o$ site results in elevated $O_2^{\bullet-}$ formation, we postulate that mutations in the cyt *b* protein, causing obstruction of the proximal $Q_o$ site, but leaving the distal $Q_o$ site functionally intact, will lead to abnormally elevated levels of $O_2^{\bullet-}$ production in the uninhibited cyt $bc_1$ complex. We note that mutations in mitochondria-encoded genes are thought to accumulate during the aging process (*45*) and that several mutations which fit this description have already been identified in the medical literature (*46*−*48*).

## ACKNOWLEDGMENT

We thank Drs. Di Xia and Edward Berry for release of molecular coordinates and for important discussions. We thank Dr. Bernard Trumpower for advice in the purification of the yeast cyt $bc_1$ complex and Dr. Antony R. Crofts for the gift of mucidin and famoxadone, as well as stimulating conversations. We thank Dr. Kevin Walker for useful discussions.

## REFERENCES

1. Trumpower, B. L., and Gennis, R. B. (1994) *Annu. Rev. Biochem. 63*, 675−716.
2. Berry, E. A., Guergova-Kuras, M., Huang, L.-S., and Crofts, A. R. (2000) *Annu. Rev. Biochem. 69*, 1005−1075.
3. Zhang, Z., Huang, L., Shulmeister, V. M., Chi, Y. I., Kim, K. K., Hung, L. W., Crofts, A. R., Berry, E. A., and Kim, S. H. (1998) *Nature 392*, 677−684.
4. Link, T. A., Haase, U., Brandt, U., and Jagow, G. v. (1993) *J. Bioenerg. Biomembr. 25*, 221−232.
5. Crofts, A., Berry, E., Kuras, R., Guergova-Kuras, M., Hong, S., and Ugulava, N. (1999) in *Photosynthesis: Mechanisms and Effects* (Garab, G., Ed.) pp 1481−1486, Kluwer Academic Publishers, Dordrecht, The Netherlands.
6. von Jagow, G., and Link, T. A. (1986) *Methods Enzymol. 126*, 253−271.
7. von Jagow, G., and Ohnishi, T. (1985) *FEBS Lett. 185*, 311−315.
8. Bowyer, J. R., Edwards, C. A., Ohnishi, T., and Trumpower, B. L. (1982) *J. Biol. Chem. 257*, 8321−8330.
9. Thierbach, G., Kunze, B., Reichenbach, H., and Höfle, G. (1984) *Biochim. Biophys. Acta 765*, 227−235.
10. Brandt, U., Schagger, H., and von Jagow, G. (1988) *Eur. J. Biochem. 173*, 499−506.
11. Subik, J., Behun, M., Smigan, P., and Musilek, V. (1974) *Biochim. Biophys. Acta 343*, 363−370.
12. Sedmera, P., Musilek, V., Nerud, F., and Vondracek, M. (1981) *J. Antibiot. 34*, 1069.
13. Jordan, D. B., Kranis, K. T., Picollelli, M. A., Schwartz, R. S., Sternberg, J. A., and Sun, K. M. (1999) *Biochem. Soc. Trans. 27*, 577−580.
14. Sharp, R. E., Gibney, B. R., Palmitessa, A., White, J. L., Dixon, J. A., Moser, C. C., Daldal, F., and Dutton, P. L. (1999) *Biochemistry 38*, 14973−14980.
15. Crofts, A. R., Guergova-Kuras, M., Huang, L., Kuras, R., Zhang, Z., and Berry, E. A. (1999) *Biochemistry 38*, 15791−15806.
16. Crofts, A. R., and Wang, Z. (1989) *Photosynth. Res. 22*, 69−87.
17. Mitchell, P. (1975) *FEBS Lett. 59*, 137−139.
18. Mitchell, P. M. (1976) *J. Theor. Biol. 62*, 327−367.
19. Trumpower, B. L. (1990) *J. Biol. Chem. 265*, 11409−11412.
20. Ding, H., Moser, C. C., Robertson, D. E., Tokito, M. K., Daldal, F., and Dutton, P. L. (1995) *Biochemistry 34*, 15979−15996.
21. Iwata, S., Lee, J. W., Okada, K., Lee, J. K., Iwata, M., Rasmussen, B., Link, T. A., Ramaswamy, S., and Jap, B. K. (1998) *Science 281*, 64−71.
22. Hunte, C., Koepke, J., Lange, C., Rossmanith, T., and Michel, H. (2000) *Struct. Folding Des. 8*, 669−684.
23. Gao, X., Wen, X., Yu, C., Esser, L., Tsao, S., Quinn, B., Zhang, L., Yu, L., and Xia, D. (2002) *Biochemistry 41*, 11692−11702.
24. Muller, F., Crofts, A. R., and Kramer, D. M. (2002) *Biochemistry 41*, 7866−7874.
25. Brandt, U. (1996) *Biochim. Biophys. Acta 1275*, 41−46.
26. Kramer, D. M., and Crofts, A. R. (1993) *Biochim. Biophys. Acta 1183*, 72−84.
27. Sacksteder, C. A., Kanazawa, A., Jacoby, M. E., and Kramer, D. M. (2000) *Proc. Natl. Acad. Sci. U.S.A. 97*, 14283−14288.
28. Boveris, A., and Cadenas, E. (1975) *FEBS Lett. 54*, 311−314.
29. Boveris, A. (1977) *Adv. Exp. Med. Biol. 78*, 67−82.
30. Gray, K. A., and Daldal, F. (1995) in *Anoxygenic Photosynthetic Bacteria* (Blankenship, R. E., Madigan, M. T., and Bauer, C. E., Eds.) pp 747−774, Kluwer Academic Publishers, Dordrecht, The Netherlands.
31. Kim, H., Xia, D., Yu, C. A., Xia, J. Z., Kachurin, A. M., Zhang, L., Yu, L., and Deisenhofer, J. (1998) *Proc. Natl. Acad. Sci. U.S.A. 95*, 8026−8033.

32. Pedretti, A., Villa, L., and Vistoli, G. (2002) *J. Mol. Graphics Modell. 21*, 47−49.
33. Brandt, U., Schagger, H., and von Jagow, G. (1988) *Eur. J. Biochem. 173*, 499−506.
34. Muller, F. (2000) *J. Am. Aging Assoc. 23*, 227−253.
35. Turrens, J. F., Alexandre, A., and Lehninger, A. L. (1985) *Arch. Biochem. Biophys. 237*, 408−414.
36. Iwata, M., Bjorkman, J., and Iwata, S. (1999) *J. Bioenerg. Biomembr. 31*, 169−175.
37. Kim, H., Xia, D., Yu, C. A., Xia, J. Z., Kachurin, A. M., Zhang, L., Yu, L., and Deisenhofer, J. (1998) *Proc. Natl. Acad. Sci. U.S.A. 95*, 8026−8033.
38. Brugna, M., Rogers, S., Schricker, A., Montoya, G., Kazmeier, M., Nitschke, W., and Sinning, I. (2000) *Proc. Natl. Acad. Sci. U.S.A. 97*, 2069−2074.
39. Barja, G. (1998) *Ann. N.Y. Acad. Sci. 854*, 224−238.
40. Ksenzenko, M., Konstantinov, A. A., Khomutov, G. B., Tikhonov, A. N., and Ruuge, E. K. (1983) *FEBS Lett. 155*, 19−24.
41. Starkov, A. A., and Fiskum, G. (2001) *Biochem. Biophys. Res. Commun. 281*, 645−650.
42. Raha, S., McEachern, G. E., Myint, A. T., and Robinson, B. H. (2000) *Free Radical Biol. Med. 29*, 170−180.
43. Brandt, U. (1999) *J. Bioenerg. Biomembr. 31*, 243−250.
44. Sharp, R. E., Moser, C. C., Gibney, B. R., and Dutton, P. L. (1999) *J. Bioenerg. Biomembr. 31*, 225−233.
45. Beckman, K. B., and Ames, B. N. (1999) *Mutat. Res. 424*, 51−58.
46. Andreu, A. L., Checcarelli, N., Iwata, S., Shanske, S., and DiMauro, S. (2000) *Pediatr. Res. 48*, 311−314.
47. Wibrand, F., Ravn, K., Schwartz, M., Rosenberg, T., Horn, N., and Vissing, J. (2001) *Ann. Neurol. 50*, 540−543.
48. Polyak, K., Li, Y., Zhu, H., Lengauer, C., Willson, J. K., Markowitz, S. D., Trush, M. A., Kinzler, K. W., and Vogelstein, B. (1998) *Nat. Genet. 20*, 291−293.

BI0342160